CHEMISTRY & BIODIVERSITY

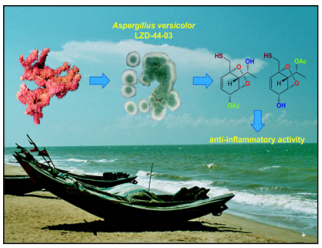

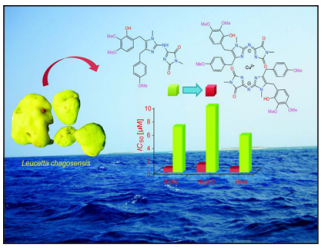

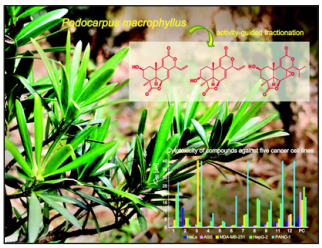

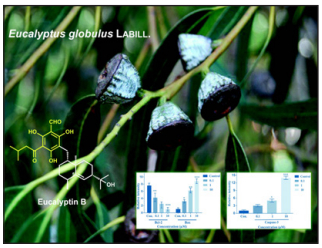

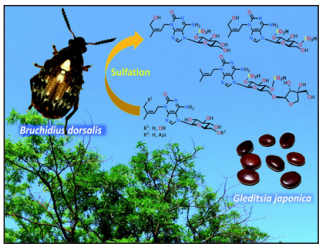

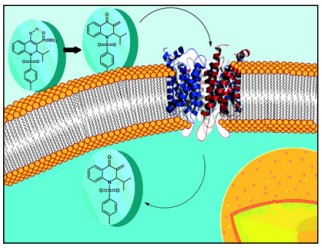

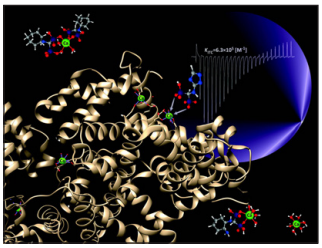

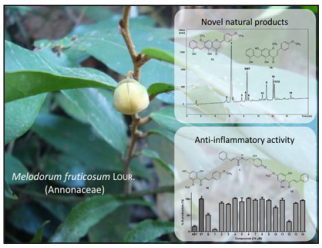

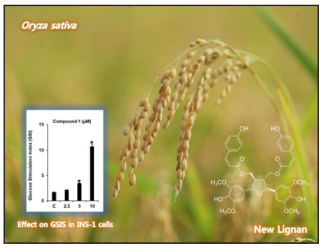

Reprint

www.cb.wiley.com

WILEY-VHCA

DOI: 10.1002/cbdv.201900028

CHEMISTRY & BIODIVERSITY

Pentafluorophenyl Substitution of Natural Di(indol-3-yl)methane Strongly Enhances Growth Inhibition and Apoptosis Induction in Various Cancer Cell Lines

Aamir Ahmad,[a] Prasad Dandawate,[b, c] Sebastian Schruefer,[d] Subhash Padhye,[b, c] Fazlul H. Sarkar,[e] Rainer Schobert,[d] and Bernhard Biersack*[d]

[a] Mitchell Cancer Institute, University of South Alabama, Mobile, Alabama 36604, USA
[b] Department of Cancer Biology, School of Medicine, KU Medical Center, Kansas City, Kansas 66160, USA
[c] ISTRA, Abeda Inamdar Senior College, Pune 411001, India
[d] Organic Chemistry Laboratory, University of Bayreuth, 95447 Bayreuth, Germany,
e-mail: bernhard.biersack@yahoo.com
[e] Retired as Distinguished Professor, Department of Pathology, Wayne State University School of Medicine, Detroit, Michigan 48201, USA

Di(indol-3-yl)methane (=3,3′-methanediyldi(1*H*-indole), DIM, **1**) is a known weakly antitumoral compound formed by digestion of indole-3-carbinol (=1*H*-indol-3-ylmethanol), an ingredient of various *Brassica* vegetables. Out of a series of nine fluoroaryl derivatives of **1**, three pentafluorophenyl derivatives **2c**, **2h**, and **2i** were identified that exhibited a two to five times greater anti-proliferative effect and an increased apoptosis induction when compared with **1** in the following carcinoma cell lines: BxPC-3 pancreas, LNCaP prostate, C4-2B prostate, PC3 prostate and the triple-negative MDA-MB-231 breast carcinoma. Compound **2h** was particularly efficacious against androgen-refractory C4-2B prostate cancer cells (IC_{50} = 6.4 μM) and **2i** against androgen-responsive LNCaP cells (IC_{50} = 6.2 μM). In addition, **2c** and **2h** exhibited distinct activity in three cancer cell lines resistant to **1**.

Keywords: indole, fluorine, 3,3′-methanediyldi(1*H*-indole), antitumor agents, apoptosis, biological activity.

Introduction

Indole-3-carbinol (=1*H*-indol-3-ylmethanol; **I3C**) is an ingredient of *Brassica* vegetables such as broccoli, cabbage, sprouts, and cauliflower. Upon digestion of these plants **I3C** gets converted to the condensation product di(indol-3-yl)methane (DIM, **1**; *Figure 1*). Both compounds show moderate efficacy against various cancer cell lines and tumors with a focus on prostate cancer.[1,2] The biological targets and modes of action of these compounds are largely known by now. Identified targets of **I3C** include p21, p27, cyclin-dependent kinases, Bax/Bcl-2, cytochrome P-450, and GADD153. Downstream cellular responses to dietary **I3C** were also explained by assuming a modification of nuclear transcription factors such as Sp1, the estrogen receptor, and the aryl hydrocarbon receptor.[3] Compound **1** displayed androgen antagonist activity and down-regulated platelet-derived growth factor D in prostate carcinoma cells.[4–6] Special formulations of **1**

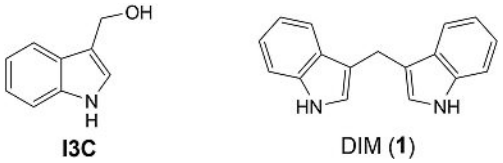

I3C DIM (**1**)

Figure 1. Chemical structures of indole-3-carbinol (**I3C**) and di(indol-3-yl)methane (**1**).

Supporting information for this article is available on the WWW under https://doi.org/10.1002/cbdv.201900028

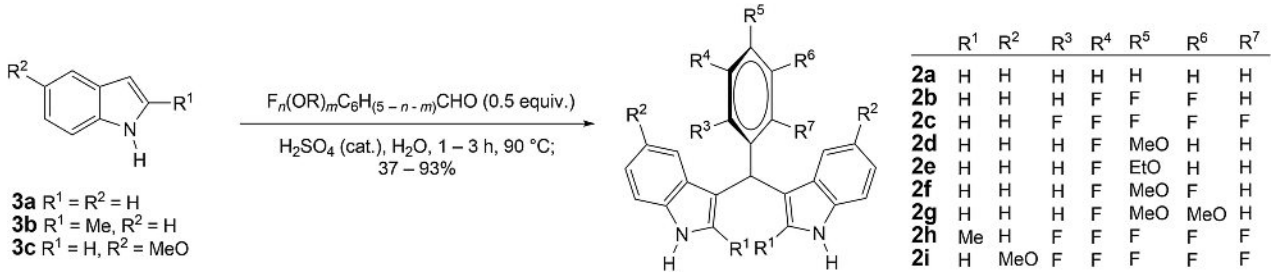

	R1	R2	R3	R4	R5	R6	R7
2a	H	H	H	H	H	H	H
2b	H	H	H	F	F	F	H
2c	H	H	F	F	F	F	F
2d	H	H	H	F	MeO	H	H
2e	H	H	H	F	EtO	H	H
2f	H	H	H	F	MeO	F	H
2g	H	H	H	F	MeO	MeO	H
2h	Me	H	F	F	F	F	F
2i	H	MeO	F	F	F	F	F

Scheme 1. Synthesis of compounds **2a**–**2i**.

led to a stabilization of the level of the prostate tumor marker protein PSA and to a partial response in prostate cancer patients.[7] In breast cancer cells **1** inhibited the nuclear translocation of NF-κB, and it induced the formation of pro-apoptotic $p27^{kip}$. **1** also augmented the efficacy of taxotere against breast cancer via NF-κB inactivation and downregulation of FoxM1.[8–11] New drugs against cancer are still sought for.[12] Safe et al. investigated a series of *para*-substituted phenyl-di(indol-3-yl)methane derivatives for their anticancer activity. The 4-fluorophenyl derivative **2a** (*Scheme 1*) showed a significantly increased efficacy and it initiated stress-mediated apoptosis in pancreatic cancer.[13] Indole-related benzimidazole derivatives were also tested for biological activities.[14] In this study we harnessed fluoroarenes as shuttle and amplifier groups for insufficiently active bisindole 'nutraceuticals'. We prepared a series of fluorophenyl substituted analogues of **1** and evaluated their apoptosis induction and anti-proliferative effects in various human cell lines including pancreatic, prostate and breast carcinoma cell lines. In addition, docking calculations were carried out for **1** and the most active new derivatives bound to putative protein targets. We have chosen COX-2 and androgen receptor because the activity of both proteins was already reported to be suppressed by **1**.[4,15] Such computational studies are customarily applied for the initial investigation of the affinity of new compounds for various protein targets.[16]

Results and Discussion

Chemistry

The compounds **2a**–**2c** were reported previously.[13,17,18] However, we used a different procedure by Gruber et al. for the synthesis of all derivatives **2a**–**2i**.[19] These were obtained as solids upon heating indoles **3a**–**3c** with half an equivalent of the corresponding fluorobenzaldehyde in water in the presence of a catalytic amount of sulfuric acid (*Scheme 1*). The compounds **2a**–**2i** were characterized by NMR, IR, and MS. The signal of the methine proton in the ^{1}H-NMR spectra of the pentafluoro derivatives **2c** (δ(H) 6.38), **2h** (δ(H) 6.32) and **2i** (δ(H) 6.21) was shifted downfield compared with the corresponding signals in the ^{1}H-NMR spectra of the other derivatives (δ(H) 5.81–5.89). The observed de-shielding can be explained by the formation of a *hydrogen* bond with the neighboring fluorine atoms in the molecules of **2c**, **2h**, and **2i**. Conversely, large highfield shifts were observed for the methine carbon signals in the ^{13}C-NMR spectra of **2c** (δ(C) 29.1), **2h** (δ(C) 29.8), and **2i** (δ(C) 29.2) compared to those of the other derivatives **2** (δ(C) 39.2–40.1). The observed shielding of the methine carbons of **2c**, **2h**, and **2i** can be explained by the high electron-density of the fluorine atoms of the phenyl ring, in particular, by the 2- and 6-F atoms.

Biological Evaluation

The anti-proliferative activity of **1** and **2a**–**2i** was first tested on cells of the triple-negative MDA-MB-231 breast cancer and the BxPC-3 pancreas cancer (*Table 1*). The pentafluorophenyl derivatives **2c**, **2h**, and **2i** were most active against MDA-MB-231 cells with IC_{50}(72 h) = 11.2–13.2 μM which is a distinct improvement over **1** (IC_{50} = 37.8 μM). Against BxPC-3 cells, **2c** reached an IC_{50}(72 h) value of 8.4 μM and **2i** displayed an IC_{50}(72 h) value of 7.5 μM and, thus, these new compounds are about four times more active than **1** (IC_{50} = 32.1 μM) in this cancer cell line. In addition, compounds **1** and **2a**–**2i** were inactive against non-malignant MCF-10A mammary and HPDE pancreas cells up to doses of 200 μM (72 h). Hence, compounds **2c**, **2h** and **2i** are also highly selective for tumor cells.

Encouraged by these results we selected the pentafluorophenyl compounds **2c**, **2h**, and **2i** for additional MTT tests on further human cancer cell lines

Table 1. Inhibitory concentrations IC_{50} (72 h, [μM]) of compounds **1** and **2a**–**2i** in MTT tests against cells of MDA-MB-231 breast and BxPC-3 pancreas carcinomas. Values are provided as means ± SD. All experiments were repeated at least three times with $n = 4$ readings in every repeat (*t*-test).

Compound	Cell line MDA-MB-231	BxPC-3
1	37.8 ± 1.1	32.1 ± 1.2
2a	19.8 ± 0.8	17.8 ± 0.7
2b	14.2 ± 0.4	12.8 ± 0.5
2c	12.9 ± 0.4	8.4 ± 0.3
2d	27.8 ± 0.9	24.1 ± 0.9
2e	17.4 ± 0.6	15.1 ± 0.6
2f	22.3 ± 1.0	18.9 ± 0.7
2g	17.8 ± 0.8	15.4 ± 0.5
2h	13.2 ± 0.6	11.8 ± 0.4
2i	11.2 ± 0.4	7.5 ± 0.3

Table 2. Inhibitory concentrations IC_{50} (72 h; [μM]) of compounds **1**, **2c**, **2h**, and **2i** in MTT tests against cells of LNCaP, C4-2B, and PC3 prostate carcinomas, 518A2 melanoma, vinblastine-resistant KB-V1/Vbl cervix carcinoma, and HT-29 colon carcinoma (n.d.: not determined). Values are provided as means ± SD. All experiments were repeated at least three times with $n = 4$ readings in every repeat (*t*-test).

Cell line	Compound **1**	**2c**	**2h**	**2i**
LNCaP	18.9 ± 0.5	8.1 ± 0.3	8.1 ± 0.2	6.2 ± 0.2
C4-2B	32.4 ± 1.0	13.1 ± 0.5	6.4 ± 0.1	n.d.
PC3	25.2 ± 0.9	12.9 ± 0.2	13.1 ± 0.3	n.d.
518A2	> 100	12.6 ± 0.3	10.7 ± 0.3	16.5 ± 0.9
KB-V1/Vbl	> 100	11.3 ± 1.2	10.9 ± 2.4	11.7 ± 0.8
HT-29	> 100	11.7 ± 2.8	9.6 ± 0.3	10.7 ± 2.1

(*Table 2*). Three prostate cancer cell lines LNCaP (AR^+, androgen-responsive), the bone metastatic LNCaP derivative C4-2B (AR^+, androgen-refractory), and PC3 (AR^-) as well as aggressive and/or drug-resistant cancer cell lines 518A2 (melanoma), KB-V1/Vbl (vinblastine-resistant cervix carcinoma) and HT-29 (colon carcinoma) were selected for these tests. The latter three cell lines are highly resistant to **1** ($IC_{50} > 100$ μM). In all cell lines the pentafluorophenyl derivatives **2c**, **2h**, and **2i** performed generally better than **1**. Compound **2h** was even five times more efficacious than **1** with $IC_{50} =$ 6.4 μM against the C4-2B cancer cells. Both **2c** and **2h** were also about twice as active as **1** against LNCaP (AR^+) cells ($IC_{50} = 8.1$ μM) and against PC3 (AR^-) cells (IC_{50} ca. 13 μM). Compound **2i** exhibited comparable activity against LNCaP cells. Further to this, the anticancer active derivatives **2c**, **2h**, and **2i** were tested in the aggressive and/or drug-resistant human cancer cell lines 518A2, KB-V1/Vbl and HT-29. In contrast to **1**, the pentafluorophenyl derivatives **2c**, **2h**, and **2i** displayed distinct growth inhibition in all three cancer cell lines ($IC_{50} = 9.6$–16.5 μM) and, thus, were able to overcome the pronounced resistance of these cancer cells towards **1**.

Finally, the compounds **1**, **2c**, and **2h** were selected for the evaluation of apoptosis induction in the three prostate cancer cell lines (*Figure 2*). Histone/DNA ELISA assays were carried out in order to determine the apoptosis rates of these three compounds. The apoptosis rates obtained for **2c** and **2h** were distinctly higher than the respective rates for **1** in all three cell lines. This correlates fairly well with the IC_{50} values obtained from the MTT assays.

Docking Studies

The anti-proliferative activities of compound **1** and of its congeners **2a**–**2i**, in particular those against prostate cancer cells, are likely related to the inhibition of crucial cellular proteins such as the androgen receptor (AR), and/or COX-2. Docking calculations with **1** and the derivatives **2a**–**2i** were carried out in order to identify new protein-drug interactions and binding modes of **2a**–**2i** after binding to AR or COX-2 which might explain their enhanced anticancer activity. While in both proteins **1** revealed the highest calculated binding energies (−9.0 kcal/mol for AR, −8.9 kcal/mol for COX-2) with one hydrogen bond (H-bond) established to Leu704 (AR) and two H-bonds to Tyr355 and Met522 (COX-2), the active derivative **2c** also bound with considerable energies (−8.3 kcal/mol for AR, −8.2 kcal/mol for COX-2). In contrast, docking of the active compounds **2h** and **2i** resulted in reduced binding energies (**2h**: −7.2 kcal/mol for AR, −7.4 kcal/mol for COX-2; **2i**: −7.2 kcal/mol for AR, −7.8 kcal/mol for COX-2) when compared with the other derivatives (*Table 3* and *4*). Interestingly, **2e** bound with a slightly higher energy than that of **2c** when docked to AR, while **2a** and **2f** reached or exceeded the binding energy of **2c** when docked to COX-2. Two H-bonds of **2c** (via both indole-NH moieties) to Thr755 and Pro682 of the AR were observed that might explain its high binding energy (*Figure 3*). In contrast, **2e** interacts with the AR (Arg752) via the ethoxy group of the phenyl ring. In the case of COX-2, compound **2c** bound to Gly350 via an H-bond to the NH of one indole moiety,

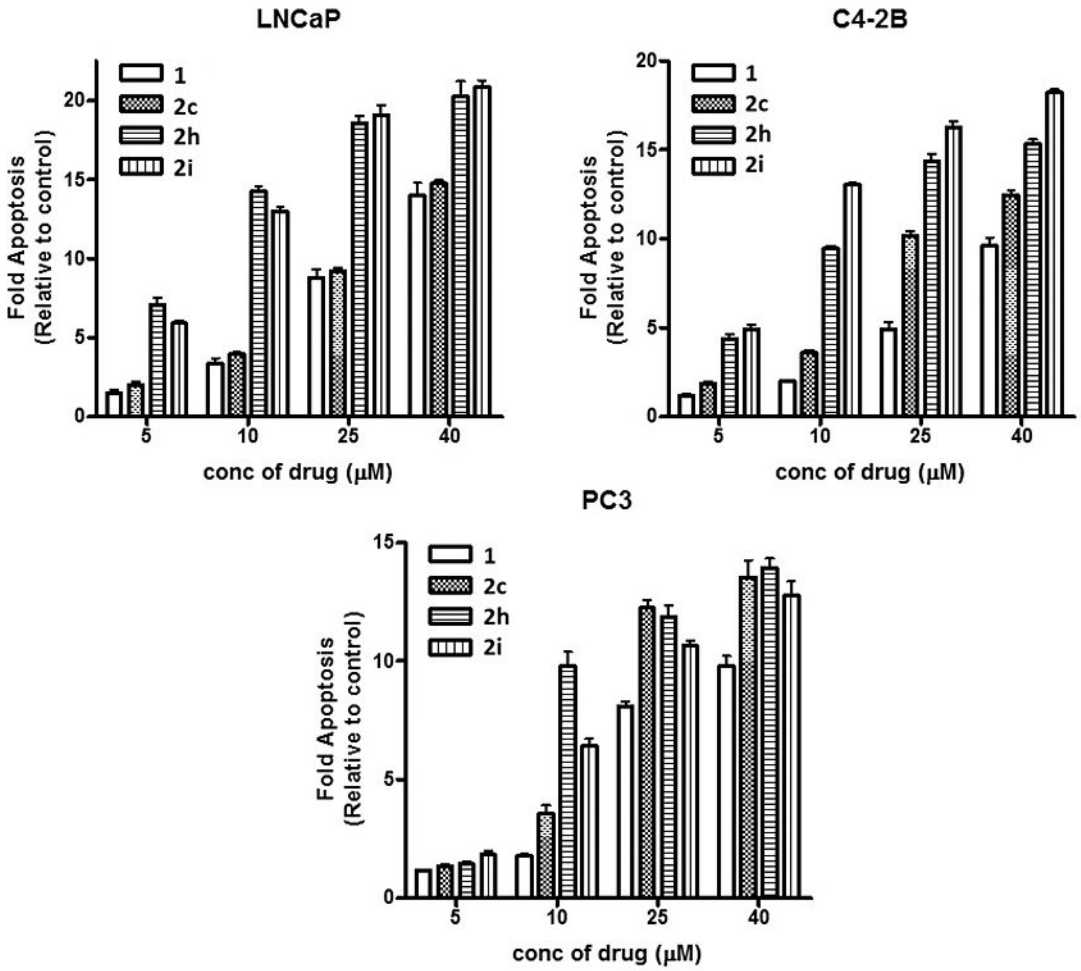

Figure 2. Apoptosis induction by **1**, **2c**, **2h**, and **2i** in LNCaP, C4-2B, and PC3 prostate carcinoma cells as detected by histone/DNA ELISA assay. The experiments were repeated three times with $n = 3$ readings in every repeat (*t*-test).

Table 3. Docking of **1** and derivatives **2a**–**2i** into the binding cavity of the androgen receptor (AR). BE = Binding energy ([kcal/mol]).

Compound	BE	No of H-bonds	Amino acid residues involved	Bond length [Å]
1	−9.0	1	LEU704	2.3
2a	−7.1	2	SER782	2.5
			GLN783	2.5
2b	−7.7	2	THR755	2.9
			PRO682	2.5
2c	−8.3	2	THR755	2.4
			PRO682	2.9
2d	−8.4	1	PHE876	2.2
2e	−8.4	1	ARG752	2.5
2f	−8.0	2	THR755	1.9
			ARG752	2.8
2g	−7.5	3	ASN756	2.0 and 3.2
			GLY683	2.0
2h	−7.2	1	GLU678	2.4
2i	−7.2	2	GLU681	2.6 and 2.8

Table 4. Docking of **1** and derivatives **2a**–**2i** into the binding cavity of COX-2. BE = binding energy ([kcal/mol]).

Compound	BE	No of H-bonds	Amino acid residues involved	Bond length [Å]
1			YR355	2.3
			MET522	2.0
2a	−8.6	1	GLN203	2.8
2b	−7.8	1	THR62	2.5
2c	−8.2	1	GLY350	2.6
2d	−7.9	2	THR62	2.4
			THR60	3.4
2e	−7.7	2	THR62	2.5
			THR60	3.5
2f	−8.2	2	THR62	2.5
			THR60	3.4
2g	−8.1	2	PHE580	2.1
			SER579	2.4
2h	−7.4	1	TYR355	1.9
2i	−7.8	3	GLN192	3.4
			ASN581	3.2
			GLN350	2.5

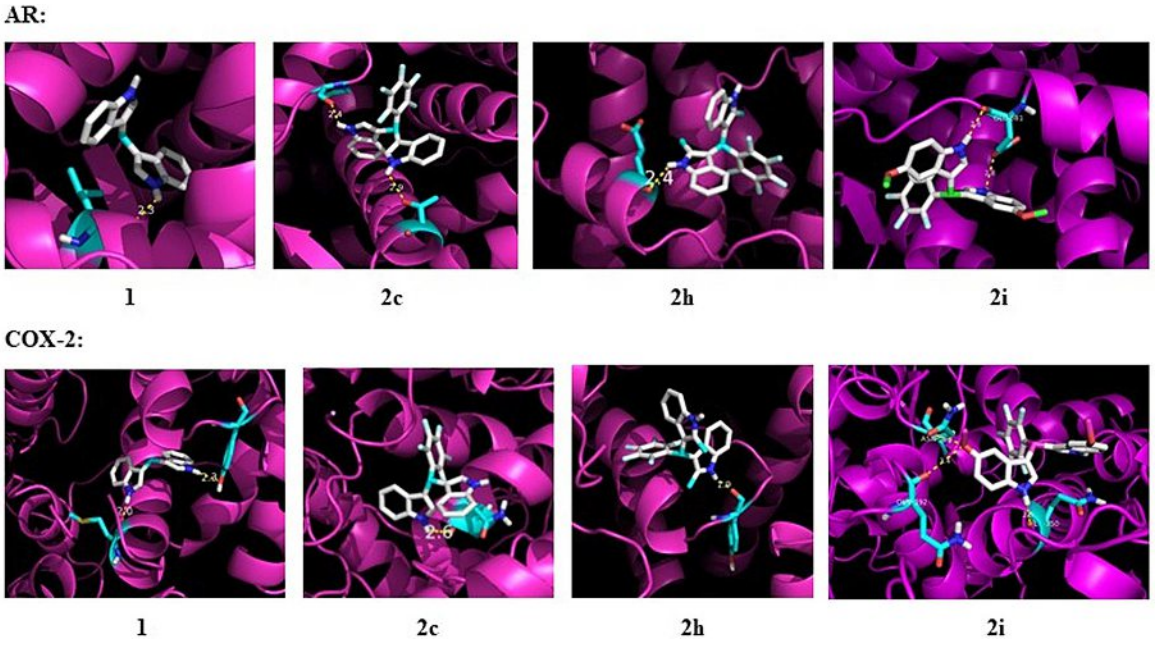

Figure 3. Proposed binding mode of **1**, **2c**, **2h**, and **2i** into the binding pockets of the androgen receptor (AR) or COX-2. Hydrogen bonds are indicated by dashed lines.

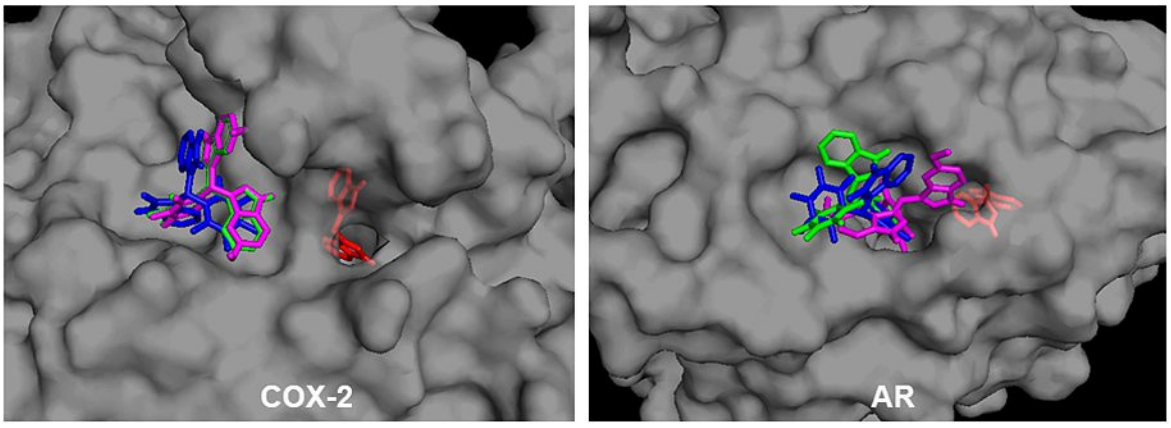

Figure 4. Overlay images of **1**, **2c**, **2h** and **2i** into the binding pockets of the androgen receptor (AR) or COX-2. Red: **1**; green: **2c**; blue: **2h**; magenta: **2i**.

while **2a** was anchored by one H-bond to Gln203 via its indole-NH. Compound **2f** bound by two H-bonds to Thr62 and Thr60 via the indole-NH and methoxyphenyl-O moieties. It is likely that the methyl groups at the indole scaffolds of **2h** impair a tight binding to the AR and to COX-2. A similar effect can be assumed for the methoxy groups at the indole moieties of compound **2i**. Yet, it is possible that an improved permeability of the cellular membranes due to the additional methyl groups of **2h** and the methoxy groups of **2i** can compensate for the reduced AR and COX-2 binding and so lead to stronger tumor cell growth inhibition when compared with **2c** and the other tested derivatives.

The nitrogen of the indole ring is mainly involved in the drug interaction with the protein cavities of COX-2 and AR. However, the binding sites of **2c**, **2h**, and **2i** differ significantly from the binding sites of **1** in both COX-2 and AR protein structures (*Figure 4*). The presence of the aromatic ring in compounds **2** is responsible for this alternative binding to both proteins. The different binding sites can explain the different activities against cancer cells.

Conclusions

A series of fluoroaryl derivatives (**2**) of di(indol-3-yl)methane (**1**) were prepared by a simple one-step protocol starting from indole derivatives **3a**–**3c** and appropriately substituted benzaldehydes. All those fluorinated compounds (**2**) that were tested on a panel of human cancer cell lines were more efficacious than **1**. The pentafluorophenyl derivatives (**2c**, **2h**, and **2i**), differing only in the substitution of the indole scaffold, were the most active compounds against the tested cancer cells. Compounds **2c** and **2h** were also strong inducers of apoptosis in prostate cancer cells. In addition, compounds **2c**, **2h**, and **2i** breached the resistance of three aggressive and drug-resistant cancer cell lines (518A2, KB-V1/Vbl, HT-29) towards **1**. This, and the obvious room for further structural fine-tuning renders the compounds **2** a promising class of test compounds.

Experimental Section

Chemistry

The starting compounds and pure solvents were purchased from the usual sources and were used without further purification. Compound **1** was provided by Dr. Michael Zeligs (BioResponse) and analyzed (NMR, IR, MS) leading to the identification of compound **1** as pure di(indol-3-yl)methane. Merck silica gel 60 (230–400 mesh) was used for column chromatography. Melting points were recorded using a Gallenkamp apparatus and are uncorrected. IR: Perkin-Elmer Spectrum One FT-IR spectrophotometer equipped with an ATR sampling unit; $\tilde{\nu}$ in cm^{-1}. NMR: Bruker Avance 300 spectrometer; δ in ppm rel. to Me_4Si as internal standard, J in Hz. EI-MS: Varian MAT 311A; in m/z (rel. %). Microanalyses indicated by the symbols of the elements were within $\pm 0.2\%$ of the theoretical values for all new compounds.

Synthesis

General Procedure for the Preparation of Bisindoles (**2**). Indole (586 mg, 5.0 mmol) was suspended in water (25 mL) and 4-fluorobenzaldehyde (276 μL, 2.5 mmol) was added. A catalytic amount of conc. sulfuric acid (3 drops) was added to the mixture before stirring at 90 °C for 2.5 h. Ethyl acetate was added to dissolve the formed precipitate, the organic phase was separated, dried over Na_2SO_4, filtered, and the filtrate was concentrated in vacuum. The residue thus obtained was purified by column chromatography (silica gel 60; ethyl acetate/*n*-hexane 1 : 2 (v/v)).

3,3′-(Phenylmethanediyl)di(1*H*-indole) (**2a**).Yield: 800 mg (2.35 mmol, 84%). IR: 3406, 1601, 1504, 1455, 1417, 1337, 1214, 1155, 1123, 1092, 1038, 1009, 853, 816, 793, 782, 738. ^{1}H-NMR (300 MHz, $CDCl_3$): 5.89 (1 H, s), 6.5–6.6 (2 H, m), 6.9–7.1 (4 H, m), 7.2–7.3 (6 H, m), 7.4–7.5 (2 H, m), 7.73 (2 H, s). ^{13}C-NMR (75.5 MHz, $CDCl_3$): 39.3, 111.1, 114.7, 15.0, 119.2, 119.3, 119.7, 121.9, 123.5, 126.8, 129.9, 130.0, 136.6, 139.6, 159.7, 162.9. EI-MS: 340 (M^+; 100), 245 (62) 223 (26) 122 (15).

Biological Studies

Cell Lines and Culture Conditions. BxPC-3 pancreas cancer (gemcitabine-sensitive) and MDA-MB-231 breast cancer cells (triple-negative) were purchased from the American Type Culture Collection (Manassas, VA) and maintained in Dulbecco's modified Eagle's medium (DMEM; Invitrogen, Carlsbad, CA) supplemented with 10% fetal calf serum (FCS), 100 U/mL of penicillin, and 100 μg/mL of streptomycin. Prostate cancer cell lines PC3 (AR^-), LNCaP (AR^+, androgen-sensitive) and C4-2B (AR^+, androgen-refractory) were obtained from the American Type Culture Collection (Manassas, VA) and maintained in RPMI 1640 (Invitrogen, Carlsbad, CA) supplemented with 10% fetal bovine serum (FBS), 100 U/mL of penicillin and 100 μg/mK of streptomycin. All cells were cultured in a humidified 5% CO_2 atmosphere at 37 °C. The human melanoma cell line 518A2 (Department of Radiotherapy and Radiobiology, University Hospital Vienna), the human colon adenocarcinoma cell line HT-29 (German Center of Biological Materials, Braunschweig, Germany), and the KB-V1/Vbl cervix cancer cell line (German Center of Biological Materials, Braunschweig, Germany) were grown in DMEM or RPMI (HT-29) medium, supplemented with 10% fetal bovine serum (FBS), 1% Antibiotic-Antimycotic solution (both from Gibco) and 250 μg/mL gentamycin (SERVA). MCF-10A breast epithelial cells were obtained from ATCC and maintained in DMEM-F12 medium supplemented with 0.1 μg/mL cholera toxin, 0.02 μg/mL epidermal growth factor, 10 μg/mL insulin, 0.5 μg/mL hydrocortisone, 100 U/mL penicillin, 100 μg/mL streptomycin and 5% horse serum in a humidified 5% CO_2 atmosphere at 37 °C. HPDE human pancreatic ductal epithelial cells were obtained from the M. D. Anderson Cancer Center of the University of Texas and maintained in RPMI-1640 media supplemented with 10% fetal bovine serum and 1% penicillin and streptomycin.

MTT Assay. MTT (=3-(4,5-dimethylthiazol-2-yl)-2,5-diphenyl-2*H*-tetrazolium bromide; ABCR) was used to identify viable cells which reduce it to a violet formazan. Cells (3×10^3/well) were seeded and cultured for 24 h on 96-well microplates. Incubation (5% CO_2, 95% humidity, 37 °C) of cells following treatment with the test compounds (dilution series from 5–40 μM in DMSO) was continued for 72 h. 25 μL of an MTT stock solution, containing 5 mg/mL in phosphate-buffered saline (PBS), was added to a final concentration of 0.05% and incubated for further 2 h at 37 °C. The supernatant was withdrawn and the formazan was dissolved in isopropanol or DMSO (100 μL). The absorbance at 595 nm was measured on an Ultra Multifunctional Microplate Reader (Tecan, Durham, NC). All experiments were repeated at least three times with quadruplet observations in every repeat.

Histone/DNA-ELISA Apoptosis Assay. The Cell Death Detection Kit (Roche, Palo Alto, CA) was used to detect apoptosis in LNCaP, C4-2B, and PC3 prostate cancer cells treated with test compounds as described previously.[20] Briefly, cells were treated with test compounds for 72 h. The cytoplasmic histone/DNA fragments from these cells were extracted and incubated in microtiter plate modules coated with anti-histone antibodies. Subsequently, the peroxidase-conjugated anti-DNA antibodies were used for the detection of immobilized histone/DNA fragments followed by color development with 2,2′-azino-bis(3-ethylbenzthiazoline-6-sulfonic acid (ABTS) substrate for peroxidase. The absorbance of the samples was determined with the microplate reader at 405 nm.

Docking Studies. All the docking calculations were performed with AutoDock Vina software to study interactions of compounds with the binding site of COX-2 (PDB ID: 6COX) and androgen receptor (PDB ID: 1E3G).[21] The 3D molecular structures of the compounds were generated by CORINA software. Compounds were energy minimized to obtain stable conformation of bonds and angles in MGL tools. The molecular docking was performed to obtain a population of possible conformations and orientations for the ligands at the binding site. All molecular docking studies were carried out in AutoDock Vina software by creating grid with $60\times60\times60$ and grid center defined with x, y, and z axis by implementing Lamarckian Genetic Algorithm (LGA). The best conformation was chosen with the most negative binding energy after docking. The interactions of compounds with COX-2 and androgen receptor binding sites including hydrogen bonds and the bond lengths were analyzed using PyMOL software.[22]

Author Contribution Statement

A. A. and S. S. designed and performed the biological assays. B. B. synthesized the test compounds and wrote the article. P. D. performed the docking calculations. S. P., F. H. S., and R. S. contributed to the study design, interpretation of the data and the drafting of the manuscript.

References

[1] R. K. Tiwari, L. Guo, H. L. Bradlow, N. T. Telang, M. P. Osborne, 'Selective responsiveness of human breast cancer cells to indole-3-carbinol, a chemopreventive agent', *J. Natl. Cancer Inst.* **1994**, *86*, 126–131.

[2] C. Hong, H. A. Kim, G. L. Firestone, L. F. Bjeldanes, '3,3′-Diindolylmethane (DIM) induces G(1) cell cycle arrest in human breast cancer cells that is accompanied by Sp1-mediated activation of p21 (WAF1/CIP1) expression', *Carcinogenesis* **2002**, *23*, 1297–1305.

[3] Y. S. Kim, J. A. Milner, 'Targets for indole-3-carbinol in cancer prevention', *J. Nutr. Biochem.* **2005**, *16*, 65–73.

[4] H. T. Le, C. M. Schaldach, G. L. Firestone, L. F. Bjeldanes, 'Plant-derived 3,3′-diindolylmethane is a strong androgen antagonist in human prostate cancer cells', *J. Biol. Chem.* **2003**, *278*, 21136–21146.

[5] D. Kong, S. Banerjee, W. Huang, Y. Li, Z. Wang, H. R. Kim, F. H. Sarkar, 'Mammalian target of rapamycin repression by 3,3′-diindolylmethane inhibits invasion and angiogenesis in platelet-derived growth factor-D-overexpressing PC3 cells', *Cancer Res.* **2008**, *68*, 1927–1934.

[6] C. V. Ustach, H.-R. C. Kim, 'Platelet-derived growth factor D is activated by urokinase plasminogen activator in prostate carcinoma cells', *Mol. Cell. Biol.* **2005**, *25*, 6279–6288.

[7] F. H. Sarkar, Y. Li, 'Harnessing the fruits of nature for the development of multi-targeted cancer therapeutics', *Cancer Treat. Rev.* **2009**, *35*, 597–607.

[8] K. M. W. Rahman, F. H. Sarkar, 'Inhibition of nuclear translocation of nuclear factor-κB contributes to 3,3′-diindolylmethane-induced apoptosis in breast cancer cells', *Cancer Res.* **2005**, *65*, 364–371.

[9] Z. Wang, B. W. Yu, K. M. W. Rahman, F. Ahmad, F. H. Sarkar, 'Induction of growth arrest and apoptosis in human breast cancer cells by 3,3′-diindolylmethane is associated with induction and nuclear localization of $p27^{kip'}$', *Mol. Cancer Ther.* **2008**, *7*, 341–349.

[10] K. M. W. Rahman, S. Ali, A. Aboukameel, S. H. Sarkar, Z. Wang, P. A. Philip. W. A. Sakr, A. Raz, 'Inactivation of NF-κB by 3,3′-diindolylmethane contributes to increased apoptosis induced by chemotherapeutic agent in breast cancer cells', *Mol. Cancer Ther.* **2007**, *6*, 2757–2765.

[11] A. Ahmad, S. Ali, Z. Wang, S. S. Ali, S. Sethi, W. A. Sakr, A. Raz, K. M. W. Rahman, '3,3′-Diindolylmethane enhances

taxotere-induced growth inhibition of breast cancer cells through downregulation of FoxM1', *Int. J. Cancer* **2011**, *129*, 1781 – 1791.
[12] K. Sampath, C. Jayabalakrishnan, 'Ruthenium(III) thiosemicarbazone complexes: synthesis, characterization, DNA binding, antibacterial, in vitro anticancer and antioxidant studies', *DJ J. Eng. Chem. Fuel* **2016**, *1*, 40 – 53.
[13] P. Lei, M. Abdelrahim, S. D. Cho, X. Liu, S. Safe, 'Structure-dependent activation of endoplasmic reticulum stress mediated apoptosis in pancreatic cancer by 1,1-bis(3′-indoly)-1-(p-substituted phenyl)methanes', *Mol. Cancer Ther.* **2008**, *7*, 3363 – 3372.
[14] J. Jayabharati, V. Thanikachalam, K. Jayamoorthy, 'Antioxidant benzimidazole bind bovine serum albumin', *J. Photochem. Photobiol. B* **2012**, *115*, 85 – 92.
[15] S. Y. Park, E. J. Kim, I.-J. Kang, Y.-H. Kang, H. K. Shin, J. H. Y. Park, 'Inhibition of phorbol ester-induced COX-2 expression by 3,3′-diindolylmethane (DIM) in human mammary epithelial cells', *FASEB J.* **2007**, *21*, A1.
[16] J. I. Ahamed, V. Panjanathan, K. Perinbam, K. S. Meena, 'Synthesis and computational studies of 2-nitro-3-phenyl-3-(phenylthio)propan-1-ol and their derivatives', *DJ J. Eng. Chem. Fuel* **2017**, *2*, 9 – 24.
[17] S. Chandrasekhar, S. Khatun, G. Rajesh, C. R. Reddy, 'B $(C_6F_5)_3$: an efficient catalyst for reductive alkylation of alkoxy benzenes and for synthesis of triarylmethanes using aldehydes', *Tetrahedron Lett.* **2009**, *50*, 6693 – 6697.
[18] S. Fujii, H. Kimoto, M. Nishida, L. A. Cohen, 'Synthesis of 1-(pentafluorophenyl)-β-carboline', *J. Fluorine Chem.* **1990**, *46*, 479 – 489.
[19] D. Maciejewska, M. Rasztawicka, I. Wolska, E. Anuszewska, B. Gruber, 'Novel 3,3′-diindolylmethane derivatives: synthesis and cytotoxicity, structural characterization in solid state', *Eur. J. Med. Chem.* **2009**, *44*, 4136 – 4147.
[20] A. Ahmad, S. Banerjee, Z. Wang, D. Kong, F. H. Sarkar, 'Plumbagin-induced apoptosis of human breast cancer cells is mediated by inactivation of NF-κB and Bcl-2', *J. Cell. Biochem.* **2008**, *105*, 1461 – 1471.
[21] O. Trott, A. J. Olson, 'AutoDock Vina: improving the speed and accuracy of docking with a new scoring function, efficient optimization, and multithreading', *J. Comput. Chem.* **2010**, *31*, 455 – 461.
[22] W. L. DeLano, 'Pymol: An open-source molecular graphics tool', in 'CCP4 Newsletter on Protein Crystallography', 2002, Number 40, pp. 44 – 53.

Received January 15, 2019
Accepted February 4, 2019

